

Backward surface waves at photonic crystals

S. Foteinopoulou,^{1,2} M. Kafesaki,^{1,3} E. N. Economou,^{1,4} and C. M. Soukoulis^{1,2,3}

¹*Institute of Electronic Structure and Laser (IESL), Foundation of Research and Technology-Hellas (FORTH), Heraklion, Crete 71110, Greece*

²*Ames Laboratory-USDOE, and Department of Physics and Astronomy, Iowa State University, Ames, Iowa 50011, USA*

³*Department of Materials Science and Technology, University of Crete, Heraklion, Crete 71003, Greece*

⁴*Department of Physics, University of Crete, Heraklion, Crete 71003, Greece*

(Received 31 October 2006; revised manuscript received 22 February 2007; published 19 June 2007)

We investigate wave propagation with opposite energy and phase velocity at the surface of a two-dimensional photonic crystal. We introduce a surface defect based on a terminating row rich in material. We show how this type of defect induces surface modes with dispersion that can be flexibly manipulated. We observe the formation of single or multiple surface bands coming from the upper periodic band with a negative or a positive band slope. We perform a numerical experiment, realizable at mid- and near-infrared frequencies, which unambiguously verifies in a direct fashion the forward or backward type of propagation of the excited surface wave. Our numerical results demonstrate the existence of backward-propagating surface waves stemming from bands with a negative slope. This study may aid the design of subdiffraction plasmon based guiding devices.

DOI: [10.1103/PhysRevB.75.245116](https://doi.org/10.1103/PhysRevB.75.245116)

PACS number(s): 42.70.Qs, 78.20.Ci, 41.20.Jb, 42.25.-p

The advent of photonic crystal (PC) materials^{1,2} spurred a lot of interest toward the existence of surface modes at the interfaces of such materials.³⁻⁶ These modes remain localized around the PC surface in a manner similar to surface plasmons on metal slabs.⁷ The first experimental observation of such photonic crystal surface waves came by Robertson *et al.*³ In the experiment, the authors employed a standard attenuated total reflection setup, widely used for surface-plasmon observations on metals.⁸ The majority of the subsequent theoretical studies focused on the existence of such surface modes in various PC structures. It was found that the frequency and in many cases even the mere existence of PC surface waves are strongly influenced by the way the periodic PC is terminated.^{2,4,5} Nevertheless, the initial acute interest for PC surface modes had somewhat subsided until recently. The need to understand and engineer PC surface modes came back to light, when these deemed to play a key role in newly discovered PC phenomena. In particular, it was found that PC surface modes can strongly influence the subdiffraction focusing properties of PC-based slab superlenses.⁹⁻¹¹ Moreover, coupling to such surface states in PC subwavelength-width waveguides leads to a highly directional exit beam.¹²⁻¹⁴

Despite the intensive research on PC surface phenomena,³⁻⁶ one aspect of the PC surface-wave propagation remains unexplored. In negative index metamaterials, uniform¹⁵ or composite¹⁶⁻¹⁸ energy and phase propagate in opposite direction, a phenomenon known as backward wave propagation.^{19,20} Recent studies showed that under certain conditions,²¹ photonic crystals can behave in many respects like the Veselago¹⁵ negative index medium,²²⁻²⁴ thus supporting backward wave propagation. A backward type of propagation inside a PC or other left-handed media can be identified experimentally only indirectly by observing the transmitted field distribution through a material-wedge structure.^{23,25} It is certainly most interesting to search for backward-propagating PC surface modes. First, the directionality of the modes is pertinent to surface-plasmon-based

guiding structures²⁶ and related optical devices. But more importantly, the possibility of the electromagnetic field detection around the PC surface with a local probe enables the direct demonstration of the backward wave propagation phenomenon.

In this paper, we investigate numerically the existence of backward surface waves at the surface of a photonic crystal. We propose an experimental setup, realizable at both microwave and visible frequencies, which unambiguously verifies in a direct fashion the type of PC surface-wave propagation (forward or backward). We create the PC surface mode through a defect row located at the PC surface.^{26,27} We employ a surface defect consisting of a one-dimensional lattice with a basis of two or more elements. Such complex type of defect, with structural elements identical to the bulk-PC sites, holds many advantages. In fact, it involves many modifiable parameters to permit flexible manipulation of the surface mode and provides routes for PC-surface-mode dispersion engineering. Furthermore, patterning these types of surface defects on mid- and near-infrared PC structures^{28,29} is much easier than patterning a surface row with specific termination.²⁻⁵

We search for surface modes at the surface of a square two-dimensional PC, consisting of cylindrical alumina ($\epsilon=9.3$) pillars in air, with radius $r=a/6$, with a being the lattice constant. We take the electric field to be parallel to the pillars [E (TM) polarization]. We employ a two-dimensional finite difference frequency domain³⁰ (FDFD) technique based on the solution of Helmholtz's equation on a spatial grid lattice.³¹ The application of Bloch boundary conditions yields a solvable $N \times N$ system of equations, where N represents the total number of grid points within the numerical lattice. This system can be transformed into a generalized eigenvalue equation problem. The eigenvalues provide the dispersion relation $\omega(k_{\parallel})$, where k_{\parallel} represents the wave vector along the PC surface and perpendicular to the pillars. Conversely, the eigenvector for a specific eigenvalue, $\omega(k_{\parallel})$,

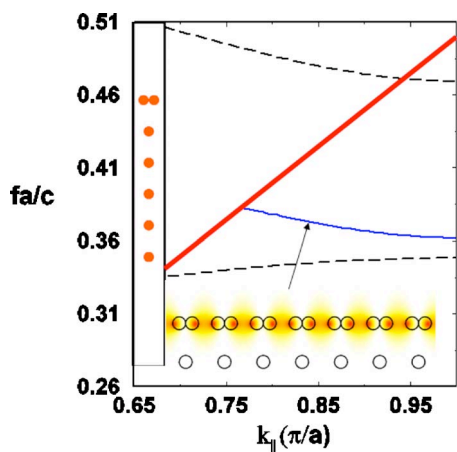


FIG. 1. (Color online) Band dispersion for a surface mode (solid line) corresponding to a PC with surface corrugation based on a dimer surface defect, as depicted in the left inset. The vertical axis represents the frequency in dimensionless units (fa/c). The PC surface mode lies below the lightline (bold straight line) and within the band gap which spans the frequency region between the dashed lines. The field plot in the lower inset depicts the spatial field distribution belonging to the mode indicated with the arrow. We plot the square of the electric field’s absolute value around the PC surface, where the field values are significant.

gives the field profile of the corresponding mode. We note that the presence of the surface breaks the translational symmetry in the normal direction. Accordingly, we must consider a supercell⁵ that spans the entire FDFD computational domain. This supercell consists of only one unit cell along the lateral direction, where translational symmetry still applies. Nevertheless, several PC sites (including the defect) embedded in air should be taken along the normal direction. The number of sites, as well as the length of the air space on the top and bottom of the terminating PC sites, must be sufficient³² to disallow any mode coupling between the top and bottom PC row. In all the subsequent calculations, the computational space is discretized with a grid cell $a/21 \times a/21$ large.

We first explore a type of a surface defect which can be formed by substituting each site on the upper PC row with a dimer, composed of pillars identical to the pillars of the bulk PC and oriented along the lateral direction. We show the corresponding supercell used in the FDFD method in the left inset of Fig. 1. We find one PC-surface-mode band indicated with the solid line in the figure. The straight line represents the lightline, and the dashed lines the limits of the first and second band of the periodic PC. As expected, the surface mode lies below the lightline and within the band gap. For a specific value of the wave vector k_{\parallel} indicated with the arrow, we also plot the spatial distribution of the electric field squared in the lower inset of Fig. 1. Indeed, we observe high field values and confinement around the surface. It should be noted that our FDFD calculations reveal that the surface mode shown in Fig. 1 is pulled down from the second band (air band). On the other hand, we checked that defects arising from a material deficient³³ upper row in the same type of periodic PC are pushed up from the first band (dielectric band). In other words, PC surface modes act like bulk-PC

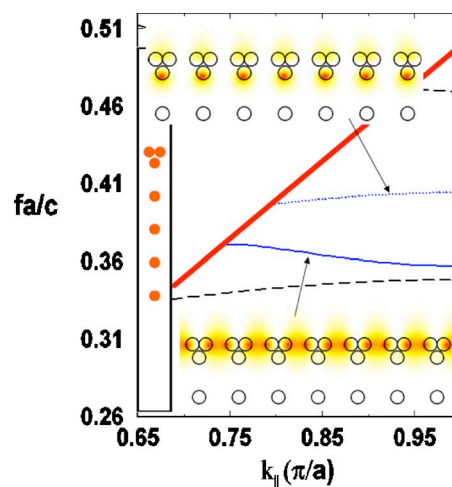


FIG. 2. (Color online) Same as in Fig. 1 but when the dimer-defect approaches the first PC row to form a three-pillar defect, as seen in the inset. Two PC-surface-mode bands with opposite band slopes are found. The field distributions correspond to two indicative modes belonging to each of these bands.

defects with the addition or removal of material. The surface band shown in Fig. 1 arises from the addition of alumina at the surface and is thus analogous to semiconductor donor states.^{2,34}

It is interesting to examine how the surface band shown in Fig. 1 can be tuned. In the corresponding dimer type of defect, the distance between the defect row and the rest of the bulk PC equals one lattice constant, a . We can modify this distance or alter the separation between the two pillars composing the dimer defect or both. Our calculations show that as the separation between the dimer cylinders increases, the surface band drops in frequency until it touches the upper limit of the first band. For large k_{\parallel} , the mode practically coincides with the periodic PC band edge.³⁵

Now, we investigate the surface-band behavior as the distance between the dimer defect and the periodic PC shortens. To be specific, we take the defect-PC separation equal to $a/2$ and find a surface band with negative slope similar to the one shown in Fig. 1 but also a second nonmonotonic band at lower frequencies. If we decrease further the separation to $a/3$, we find again two bands: one with negative slope like the one in Fig. 1 and one with positive slope appearing at higher frequencies. We plot the results in Fig. 2 for the latter case along with the supercell taken in the FDFD method. Note that the defect row in this case has touched the first row of the periodic PC. Thus, it forms a composite defect together with the first bulk-PC row. That is to say, this striking behavior of the surface band stems from a three-pillar defect, as seen in the supercell of Fig. 2. We also depict the field distributions for two different modes lying in the respective bands specified by the arrows in the figure. The spatial profile shown corresponds to the square of the magnitude of the electric field. The mode belonging to the lower PC-surface-mode band with negative slope has a substantially different configuration from the mode for the higher PC-surface-mode band with positive slope. We note that it is also entirely possible to excite laterally propagating (guided) waves

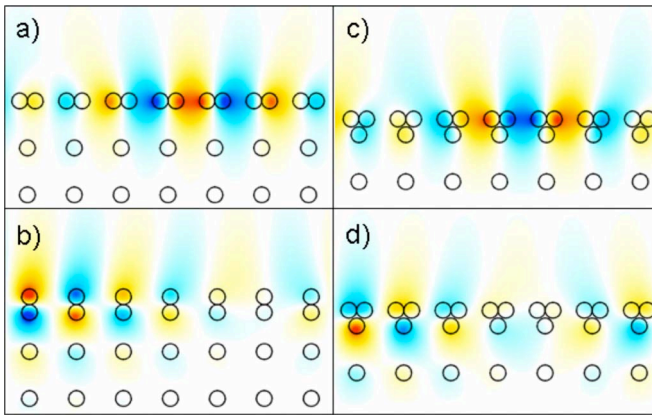


FIG. 3. (Color online) Electric field plots that correspond to different PC-surface-mode bands. Case (a) corresponds to the surface band of Fig. 1, case (b) to the band resulting from a dimer defect oriented perpendicularly to the surface, case (c) to the lower surface band of Fig. 2, and case (d) to the higher surface band of Fig. 2.

through a single array of alumina-rod dimers or trimers, even without the presence of the underlying periodic PC. These modes are analogous to waveguide modes through silver spheres³⁶ and, in some cases (as in Fig. 1), practically coincide with the PC surface modes. However, despite the concentration of the field around the top defect row, we found that the underlying periodic PC impacts in general the properties of such laterally propagating wave as these manifest themselves in the characteristics of the corresponding band dispersion.

We examine further the properties of the dimer defect and find that they also depend on the orientation of the dimer defect. By rotating the dimer axis around the surface, we find that we can induce a change in the frequency location, slope, or even the number of related surface-mode band(s). Our numerical results imply that a dimer oriented perpendicularly to the surface induces a surface mode with positive band slope that is pulled down from the air band. Surface bands reported thus far, which emanate from a material deficient terminating row, are pushed up from the dielectric band and have a positive band slope. Here, we found two distinct cases of PC-surface-mode bands which emanate from a dimer surface defect oriented laterally and normally, respectively. Both these surface bands drop from the air band but their respective slopes have opposite signs. Correspondingly, there is no correlation between the kind of surface band (donor or acceptor) and the respective slope of the band. However, the electric field maps of the surface modes in all these different cases reveal a noteworthy correlation. This is illustrated in Fig. 3 for four different cases. Figure 3(a) depicts the electric field corresponding to the surface-mode band of Fig. 1. Figure 3(b) depicts the electric field for a surface mode emanating from a dimer defect oriented perpendicularly to the PC surface. The field depicted in Figs. 3(c) and 3(d) corresponds to the lower and upper respective surface bands, which arise from the trimer-type defect of Fig. 2. We observe that the electric field of a positive-band-slope donor surface mode flips sign when crossing the mid-defect plane. On the con-

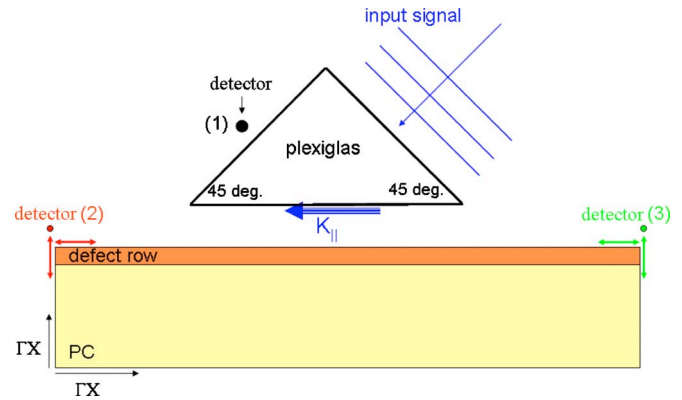


FIG. 4. (Color online) Schematics of proposed experiment implemented numerically by the finite difference time domain (FDTD) method.

trary, the electric field of a negative-band-slope donor surface mode retains its sign when crossing the mid-defect plane. It is not surprising that surface-mode field profiles with evenlike and oddlike symmetries in respect to the interface lead to bands with a different band slope. Actually, the band slope can be expressed as a function of the electric field with the aid of the $\mathbf{k} \cdot \mathbf{p}$ perturbation method.^{21,37} We found in general that evenlike modes can favor a strong negative contribution in such an expression, thus yielding a negative band slope. This is not the case with oddlike modes, which lead accordingly to a positive band slope.

In periodic PCs, previous studies^{21,23} demonstrated that a negative band slope leads to a backward-propagating Floquet-Bloch wave. In particular, the Floquet-Bloch mode gains consistently a constant phase while traveling from one unit cell to the next, throughout the photonic lattice.²¹ The sign of this phase coincides with the sign of the corresponding band slope and signifies a parallel (when positive) or antiparallel (when negative) relation between phase and energy velocities (for isotropic dispersion in wave vector space). To our knowledge, it has not been thus far demonstrated how the slope of a PC surface band relates with the type of propagation (forward or backward). In order to investigate, we propose the following experiment described in the schematics of Fig. 4. We implement such experiment in the two-dimensional finite difference time domain³⁸ (FDTD) method with perfect matched layer (PML) absorbing boundary conditions.³⁹

We place a 45° isosceles Plexiglas prism on top of the photonic crystal face with the surface defect. A Gaussian beam with a wide waist is launched from the top right side of the prism and creates an evanescent wave that can excite the surface mode. We employ a pulsed signal with central frequency tuned to be around the midgap of the periodic PC (i.e., $fa/c=0.41$). Subsequently, we monitor the time evolution of the electric field at different detector points. We then apply a fast Fourier transform⁴⁰ (FFT) to the signal at each of these points and normalize it by the respective spectrum of the source. The first detector consists of one point placed just above the middle of the left side of the Plexiglas prism, as seen in Fig. 4. In the absence of any surface states, we would expect a normalized intensity strength of about 0.90.⁴¹ Now,

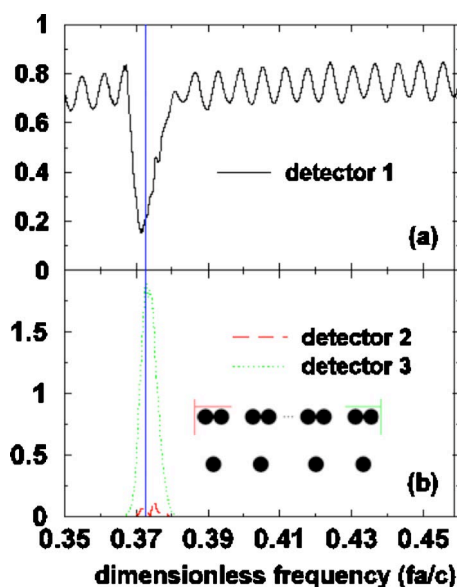


FIG. 5. (Color online) FDTD numerical experiment with the setup of Fig. 4 for the characterization of surface waves for the system of Fig. 1. The exact location of the two sets of detectors in respect to the PC is also shown in the inset. (a) Electric field intensity spectrum recorded by detector 1 (solid line). The dip signifies coupling to the surface mode. (b) Electric field intensity spectrum recorded by detector 2 (dashed line) and detector 3 (dotted line). The vertical line signifies the frequency location of the surface mode as expected from the FDFD calculations of Fig. 1 (mode which has $\frac{k_{\parallel}}{\omega/c} = n \sin 45^\circ$, with n the refractive index of Plexiglas).

when surface states are present, some power couples through the evanescent wave onto the photonic crystal and a dip would emerge in the spectrum recorded by the detector (1). The second and third set of detectors span the vicinity of the surface defects at the left and right sides of the PC structure, as seen in Fig. 4. Each set consists of monitoring points spaced $2a/21$ apart and lying on two line segments: one oriented laterally along the surface and one along the normal to the surface, as seen in Fig. 4. The respective recorded intensity represents an averaged FFT signal taken over all the detector points in each side of the PC. The collection completes after two separate FDTD runs: one recording the field on the lateral line detectors and the other on the ones oriented along the surface normal. The parallel wave vector k_{\parallel} created by the input beam points toward the left and must be conserved when the evanescent wave hits the PC surface.^{21,42} This means that a signal detected by the second set of detectors (left side) indicates a forward-propagating PC surface mode. On the other hand, a signal detected by the third set of detectors (right side) manifests the backward wave propagation for the photonic crystal surface mode. We take the length of the bottom prism face less than a half of the PC width to ensure that the signals recorded by the second and third sets of detectors will not be distorted by the prism edge.⁴³ Our numerical experiment outlined in the schematics of Fig. 4 can be realized in corresponding systems operable in microwave or infrared and visible frequencies. A monopole antenna⁹ or a scanning near-field optical microscopy (SNOM) tip¹² can serve as the localized detector probes in each side of the photonic crystal.

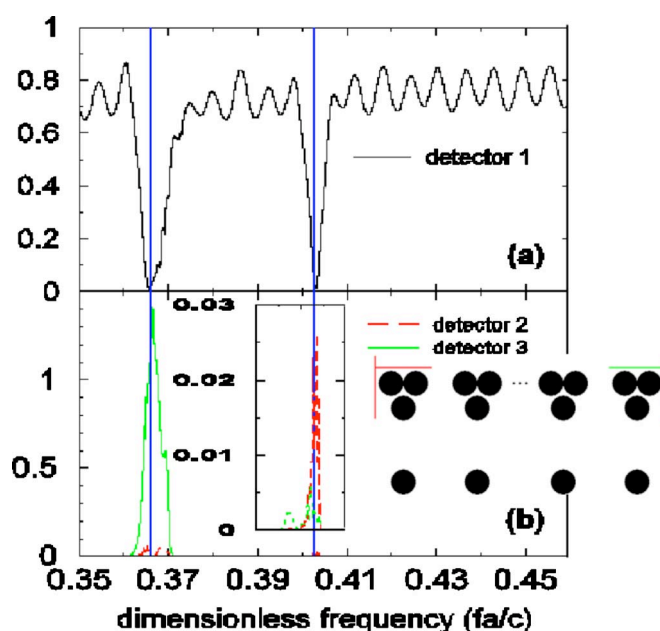


FIG. 6. (Color online) Same as in Fig. 5 for the system of Fig. 2. The signal of the second surface mode is much lower than the first. The left inset in (b) displays the signals corresponding to the second surface mode in a more appropriate scale.

We have performed the numerical FDTD experiment described above for the defect cases of Figs. 1 and 2. We plot the Fourier transformed signal arriving at the first detector in Figs. 5(a) and 6(a), respectively. Correspondingly, the signals recorded by the second and third sets of detectors are shown in Figs. 5(b) and 6(b). The exact location and size of the two line detectors in each set, at each side of the photonic crystal, are also depicted. The vertical lines in the figures designate the frequencies of the surface modes predicted previously by the FDFD method. Notice the remarkable agreement between the dips in Figs. 5(a) and 6(a) and the calculated surface-mode frequency values. Also, the signal strength around these dips is quite close to the rough estimate we just made above.⁴¹ The small discrepancy is due to the beam divergence of the finite width Gaussian beam. Now, for the case of Fig. 1, we observe a strong signal recorded by the third set of detectors at the expected frequency providing firm evidence for backward wave propagation. The enhanced intensity value of this signal in comparison with the intensity of the input beam is a lensing type of effect. We have a wide Gaussian input beam which is converted through an evanescent wave to a narrow beam tight around the dimer-defect row. We note that intensity enhancement typically can occur whenever a wide beam is focused to a narrow spot size with a lensing system.⁴⁴

We remind the reader that the PC-surface-mode band has negative slope in this case. This ascertains that similar to the case of the bulk PCs,²¹ a PC-surface-mode band with negative slope implies a backward-propagating surface wave. However, we also see in Fig. 5(b) that the second set of detectors also records a signal with strength about 5% the signal recorder by the third set of detectors. We alert the reader that by no means, this would imply a contribution of a

forward-propagating wave. After examining carefully the time evolution of all detected field, we see that all the results are caused by a superposition of a first signal caused by the initial beam, and a second signal caused by multiple reflections at the prism surfaces. It is the second signal which generates the fringes in the spectra of Figs. 5(a) and 6(a). A simple geometric ray tracing will show that this second signal contributes a k_{\parallel} same in magnitude but opposite in sign in respect to the original k_{\parallel} . Therefore, a backward surface wave excited by this second signal would arrive in the second set of detectors, hence the corresponding small signal peak. Our arguments are supported by the relative magnitude of the two signals which is consistent with a rough estimate made from Fresnel-type formulas.^{45,46} Also, the results shown in Fig. 6 establish the backward (forward) wave propagation for the first (second) mode with the negative (positive) band slope for the cases of Fig. 2. Again, the smaller humps at the same frequency are from the second multireflected signal and should not be taken into account when determining the directionality of the surface wave.

To conclude, we have investigated a dimer defect for the

surface of a two-dimensional photonic crystal consisting of the same pillars as the bulk PC. Many characteristics of this type of defect can be altered, such as separation between the dimer pillars, orientation in respect to the surface, etc., leading to flexibly engineered surface-wave bands. We identified two kinds of surface bands with a positive or a negative band slope. We have verified with a numerical experiment the existence of backward-propagating surface waves, arising from surface-wave bands with a negative band slope. Our suggested defect configuration can be implemented at corresponding structures operating at the near-IR and visible frequencies. Thus, we believe that it has potential for subdiffraction surface-plasmon-based waveguiding at these frequencies, which is recently attracting increasing attention.^{26,47,48}

This work was partially supported by Ames Laboratory (Contract No. DE-AC0207CH11385), and by EU-projects Molecular Imaging (LSHG-CT-2003-503259), Metamorphose (NoE), and Phoremest (NoE).

-
- ¹ *Photonic Band Gaps and Localization*, NATO Advanced Studies Institute, Series B: Physics, edited by C. M. Soukoulis (Plenum, New York, 1993), Vol. 308.
- ² J. D. Joannopoulos, R. D. Meade, and J. N. Winn, *Photonic Crystals: Molding The Flow of Light* (Princeton University Press, Princeton, NJ, 1995).
- ³ W. M. Robertson, G. Arjavalingam, R. D. Meade, K. D. Brommer, A. M. Rappe, and J. D. Joannopoulos, *Opt. Lett.* **18**, 528 (1993).
- ⁴ Robert D. Meade, Karl D. Brommer, Andrew M. Rappe, and J. D. Joannopoulos, *Phys. Rev. B* **44**, 10961 (1991).
- ⁵ F. Ramos-Mendieta and P. Halevi, *Phys. Rev. B* **59**, 15112 (1999).
- ⁶ J. M. Elson and P. Tran, *Phys. Rev. B* **54**, 1711 (1996).
- ⁷ N. W. Ashcroft and N. D. Mermin, *Solid State Physics* (Saunders, Philadelphia, 1976).
- ⁸ A. Otto, *Z. Phys.* **216**, 398 (1968).
- ⁹ R. Moussa, S. Foteinopoulou, Lei Zhang, G. Tuttle, K. Guven, E. Ozbay, and C. M. Soukoulis, *Phys. Rev. B* **71**, 085106 (2005).
- ¹⁰ C. Luo, S. G. Johnson, J. D. Joannopoulos, and J. B. Pendry, *Phys. Rev. B* **68**, 045115 (2003).
- ¹¹ S. Xiao, M. Qiu, Z. Ruan, and S. He, *Appl. Phys. Lett.* **85**, 4269 (2004).
- ¹² P. Kramper, M. Agio, C. M. Soukoulis, A. Birner, F. Muller, R. B. Wehrspohn, U. Gosele, and V. Sandoghdar, *Phys. Rev. Lett.* **92**, 113903 (2004).
- ¹³ Esteban Moreno, F. J. Garcia-Vidal, and L. Martin-Moreno, *Phys. Rev. B* **69**, 121402(R) (2004).
- ¹⁴ I. Bulu, H. Caglayan, and E. Ozbay, *Opt. Lett.* **30**, 3078 (2005).
- ¹⁵ V. G. Veselago, *Usp. Fiz. Nauk* **92**, 517 (1964); [*Sov. Phys. Usp.* **10**, 509 (1968)].
- ¹⁶ C. M. Soukoulis, M. Kafesaki, and E. N. Economou, *Adv. Mater.* (Weinheim, Ger.) **18**, 1941 (2006), and references therein.
- ¹⁷ G. Dolling, M. Wegener, C. M. Soukoulis, and S. Linden, *Opt. Lett.* **32**, 53 (2007).
- ¹⁸ S. Zhang, W. Fan, N. C. Panoiu, K. J. Malloy, R. M. Osgood, and S. R. Brueck, *Opt. Express* **14**, 6778 (2006).
- ¹⁹ P. A. Belov, *Microwave Opt. Technol. Lett.* **37**, 259 (2003).
- ²⁰ M. Beruete, M. Sorolla, and I. Campillo, *Opt. Express* **14**, 5445 (2006).
- ²¹ S. Foteinopoulou and C. M. Soukoulis, *Phys. Rev. B* **72**, 165112 (2005).
- ²² M. Notomi, *Phys. Rev. B* **62**, 10696 (2000).
- ²³ S. Foteinopoulou and C. M. Soukoulis, *Phys. Rev. B* **67**, 235107 (2003).
- ²⁴ S. Foteinopoulou, E. N. Economou, and C. M. Soukoulis, *Phys. Rev. Lett.* **90**, 107402 (2003).
- ²⁵ R. A. Shelby, D. R. Smith, and S. Schultz, *Science* **77**, 292 (2001).
- ²⁶ A. I. Rahachou and I. V. Zozoulenko, *J. Opt. Soc. Am. B* **23**, 1679 (2006).
- ²⁷ B. Wang, W. Dai, A. Fang, L. Zhang, G. Tuttle, Th. Koschny, and C. M. Soukoulis, *Phys. Rev. B* **74**, 195104 (2006).
- ²⁸ T. F. Krauss, in *Photonic Crystals and Light Localization in the 21st Century*, NATO Advanced Studies Institute, Series C: Mathematical and Physical Sciences, edited by C. M. Soukoulis (Kluwer, Dordrecht, 2001), Vol. 563, p. 129.
- ²⁹ U. Grüning and V. Lehmann, *Thin Solid Films* **276**, 151 (1996).
- ³⁰ C.-P. Yu and H.-C. Chang, *Opt. Express* **12**, 1397 (2004).
- ³¹ E. I. Smirnova, C. Chen, M. A. Shapiro, J. R. Sirigiri, and R. J. Temkin, *J. Appl. Phys.* **91**, 960 (2002).
- ³² The PC should be thick enough so that the field values in the last PC row are small in comparison with the field values in the top surface row. In addition, the air space on top and bottom of the PC should be sufficient to prevent the decaying fields emanating from the top defect row to hit the bottom of the PC. (The space directly above the top edge of the supercell continues directly above its bottom edge.)

- ³³The terminating upper row consists of infinite-height pillars of truncated cross section equal to 1/4, 1/2, and 3/4 of the regular circular cross section.
- ³⁴E. N. Economou, *Solid State Physics* (Crete University Press, Heraklion, Greece, 2003), Vol. 2.
- ³⁵An additional band may pull out from the second band as well but lies too close to the second PC band.
- ³⁶W. H. Weber and G. W. Ford, *Phys. Rev. B* **70**, 125429 (2004).
- ³⁷D. Hermann, M. Frank, K. Busch, and P. Wolfle, *Opt. Express* **8**, 167 (2000).
- ³⁸A. Taflove, *Computational Electrodynamics: The Finite Difference Time-Domain Method* (Artech House, Boston, 1995).
- ³⁹J.-P. Berenger, *J. Comput. Phys.* **114**, 185 (1994).
- ⁴⁰W. H. Press, B. P. Flannery, S. A. Teukolsky, and W. T. Vetterling, *Numerical Recipes: The Art of Scientific Computing* (Cambridge University Press, Cambridge, 1986).
- ⁴¹Making a rough estimate from Fresnel-type formulas, the electric field intensity at the exit of the prism should be about $[\frac{4n}{(n+1)^2}]^2$, where $n=1.60$, represents the refractive index of the prism.
- ⁴²D. Jackson, *Classical Electrodynamics* (Wiley, New York, 1999).
- ⁴³The photonic crystal edge is more than ten free space wavelengths away from the prism edge. This ensures that any near field stemming from the prism edge cannot directly influence the field in the vicinity of the PC edge.
- ⁴⁴R. Zhou, X. Chen, and W. Lu, *Phys. Rev. E* **74**, 016610 (2006).
- ⁴⁵J. P. Mathieu, *Optics* (Pergamon, New York, 1975).
- ⁴⁶A beam reflected from the second side of the prism would have an intensity $(n-1)^2/(n+1)^2 \sim 0.05$, smaller than the intensity of the beam arriving originally at the base of the prism.
- ⁴⁷J. A. Dionne, L. A. Sweatlock, H. A. Atwater, and A. Polman, *Phys. Rev. B* **72**, 075405 (2005).
- ⁴⁸A. Karalis, E. Lidorikis, M. Ibanescu, J. D. Joannopoulos, and M. Soljacčić, *Phys. Rev. Lett.* **95**, 063901 (2005).